Interplay between cancer and thrombosis; identification of key factors
Ünlü, B.

Citation
Ünlü, B. (2019, January 29). *Interplay between cancer and thrombosis; identification of key factors*. Retrieved from https://hdl.handle.net/1887/68470
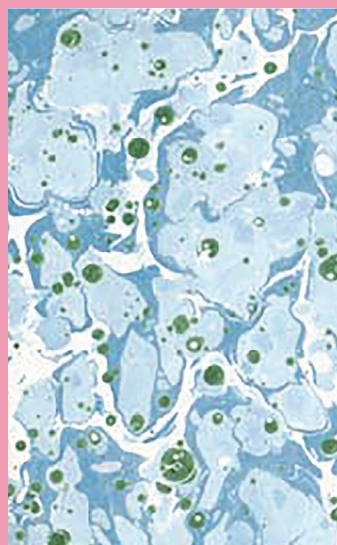
Cover Page

The handle http://hdl.handle.net/1887/68470 holds various files of this Leiden University dissertation.

Author: Ünlü, B.
Title: Interplay between cancer and thrombosis; identification of key factors
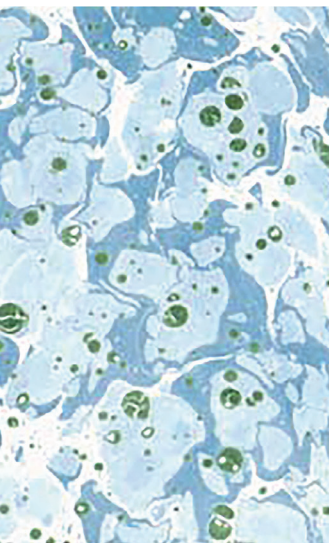**Issue Date**: 2019-01-29

Chapter 4

Integrin regulation by Tissue Factor promotes cancer stemness and metastasis in breast cancer.

Betül Ünlü
Begüm Kocatürk
Araci M. da R. Rondon
Nathalie Swier
Rob F.P. van den Akker
Erik J. Blok
Wolfram Ruf
Peter J.K. Kuppen
Henri H. Versteeg

One-sentence summary: Tissue Factor promotes early metastatic events in breast tumors by altering epithelial-to-mesenchymal transition and cancer stem cell programs through function modulation of $\beta1$ and $\beta4$ integrins.

ABSTRACT

Tissue Factor (TF) expression in breast cancer is associated with higher tumor grade, metastasis and poor survival. TF influences tumor growth through cellular signaling and that TF promotes metastasis via blood clotting. However, the role of TF signaling in metastasis has never been addressed. Here, an association between TF expression and metastasis was shown in our breast cancer cohort (N=574); and with a cancer stem cell (CSC) marker. Blockade of TF signaling inhibits metastasis 10-fold independent of primary tumor growth *in vivo*. A reduction in epithelial-to-mesenchymal transition (EMT), CSCs and expression of the pro-metastatic markers Slug and SOX9 was observed *in vitro*. Mechanistically, TF shifts from α3β1 integrin to α6β1 and α6β4 and dictates FAK recruitment, leading to reduced EMT and tumor cell differentiation. In conclusion, inhibition of TF signaling leads to a reduced EMT and CSC transcriptional programs, a reduction in primary tumor-resident CSCs and a subsequent reduction in metastasis.

INTRODUCTION

Breast cancer is the second leading cause of death in women. The lifetime-risk for breast cancer diagnosis among women is 1 in 8, with over 250.000 estimated new invasive breast cancer cases in 2017 [1]. Despite early diagnosis and improved treatment, breast cancer is still one of the leading causes of cancer-related death in women. Unfortunately, the 5-year relative survival dramatically declines to 35% in breast cancer patients with distant metastasis when compared to patients with a local tumor (98%). Nearly 40% of all breast cancer patients have regional or distant metastases, 30.8% and 6.2% respectively [1].

Prior to metastasis, tumor cells undergo epithelial-to-mesenchymal transition (EMT), in which cell-cell contact is lost and a spindle-shape morphology is acquired with enhanced migratory and invasive properties. This EMT program is accompanied by downregulation of epithelial markers (like E-cadherin) and upregulation of mesenchymal markers (e.g. Vimentin), that are under control of EMT-related transcription factors like members of the SNAIL, TWIST and ZEB families [2, 3]. After extravasation at distant organs, the reversed transition occurs, termed MET. However, it becomes more evident that there is an intimate relationship between EMT and cancer stem cells (CSCs) required for successful metastasis [4-6]. CSCs belong to the sub-population of the tumor with the ability to self-renew, seed new tumors and processing increased resistance towards chemotherapy [7]. CSCs in breast cancer may be identified based on the expression of surface markers CD133+, CD44+/CD24- and/or the intracellular protein aldehyde dehydrogenase 1 (ALDH1) [8]. The current hypotheses are either that i) cells that have undergone EMT de-differentiate into CSCs or ii) CSCs start expressing EMT-associated markers, after which they metastasize [9]. One protein that is suggested to drive cancer stemness is Tissue Factor (TF) [10].

TF is the initiator of the extrinsic coagulation pathway and is expressed on sub-endothelial cells. It binds and facilitates activation of its natural ligand factor VII (FVII) after vessel injury. This binary complex activates coagulation factor X (FX) that leads to prothrombin cleavage, activation of platelets and fibrin deposition in order to close the site of the wound. However, TF is also synthesized by breast tumor cells, and this expression has been found to associate with higher tumor grade, increased angiogenesis, reduced survival, as well as increased invasive and metastatic behavior [11].

Classically, it has been thought that TF influences tumor progression via two distinct processes. First, TF in complex with FVIIa induces i) direct cellular signaling via Protease activated Receptor-2 (PAR2) and ii) indirect TF signaling through crosstalk with integrins, to

4

promote tumor angiogenesis, tumor growth and migration, respectively. In addition, integrins also directly influence TF signaling by promoting TF-dependent PAR2 activation. TF signaling also appears to increase the invasive capacity through increased production of matrix metalloproteinases (MMPs). The latter degrade the extracellular matrix (ECM) allowing tumor cells to escape the local tumor environment. In addition, TF regulates cell adhesion and migration via integrins in a PAR2-independent manner [12, 13]. Upon entering the bloodstream, coagulant functions of TF becomes key, as it forms a fibrin/platelet-rich shield around circulating tumor cells. This prevents attack from the immune system, and thereby promotes survival of metastatic cells. PAR2-dependent signaling is facilitated by TF/β1 integrin complex assembly after binding of FVII to TF [14, 15]. So far, the role of TF signaling on the early facets of metastasis (*in vivo*) has not been addressed.

Here, we demonstrate that TF signaling, in addition to primary tumor growth, also impacts metastasis and the cellular processes underlying metastasis. Inhibition of TF signaling resulted in a downregulation of EMT-associated markers, decreased CSC activity and invasive capacity. Finally, a regulatory role for TF in integrin function and localization in cellular membrane compartments was observed, giving more insight in the mechanism underlying TF signaling-dependent metastasis.

METHODS

Reagents and cell culture

The breast cancer cell line MDA-MB-231-mfp were cultured in DMEM, supplemented with 10% fetal calf serum, 2 mM L-Glutamine (Sigma-Aldrich) and 1% penicillin/streptomycin (Gibco) in a 5% CO_2 incubator at 37 °C. To coat culture plates with ECM components vitronectin (Sigma-Aldrich) derived from human plasma and supernatant from 804G cells for laminin condition were used. For the antibody inhibition approach the flTF (Mab-10H10; mouse); β1 integrin (Mab-AIIB2; rat); PAR2 (Pab-pool7; mouse) were used.

Tissue Microarray Analysis

Tumor material from 574 non-metastasized breast cancer patients was collected who underwent tumor resection at the LUMC between 1985 and 1994 [16]. Approval was obtained from the Leiden University Medical Center (LUMC) Medical Ethics Committee. Age, tumor grade, histological type, tumor/node/metastasis status, median follow-up (17.9 years), lo-

co-regional or distant tumor recurrence and expression of ER, PgR and HER2 were known. Specimens were graded according to current pathological standards. Sections were cut and immunohistochemically stained for TF as described previously [17], including normal breast tissue of 266 patients (46%). The percentage of TF positive tumor cells was scored by two blinded observers. TF expression in breast specimens was compared to tumor recurrence and/or metastasis. Metastasis-free survival rates were calculated with the Kaplan-Meier method.

Orthotopic breast cancer cell injections into the mammary fat pad

All the animal experiments were approved by the animal welfare committee of the LUMC. All applicable institutional guidelines for the care and use of animals were followed. Orthotopic injections were performed as described previously [18]. In brief, $5x10^5$ MDA-MB-231-mfp cells were mixed with 500 µg Mab-10H10 or isotype matched mouse IgG1 (TIB115) and injected into inguinal fat pads of 6 week-old female NOD-SCID (n=4) or NOD-SCIDγ (n=5) mice (Charles River, Wilmington, MA); as an analgesic 0,05 mg/kg temgesic (Schering-Plough, Kenilworth, NJ) was injected. Sample size was selected on previous studies performed by our group [15, 17] and mice were randomly divided into two groups prior to xenograftment. The tumor dimensions were measured with a caliper and the volume was calculated with the formula $V=(LxW^2)/2$, by two independent observers. End points were when control tumors reached ~1000 mm^3 or for humane reasons defined by institutional guidelines. Primary tumors and organs were harvested and processed for further analysis. *Ex vivo* cells were isolated and cultured from tumors derived from NOD-SCID mice.

qPCR

For real time PCR analysis, total RNA was isolated using Trisure (Bioline; Bio-38033) and converted to cDNA using the Super Script II kit (Life Technologies). SYBR select (Life Technologies) was used to conduct qPCR. Primers are described in table S2. To quantify the presence of human tumor cells in mouse organs, a qPCR was performed with the housekeeping genes mouse β-actin and human GAPDH as a measure for metastasis.

Immunoprecipitation and western blotting

Prior to immunoprecipitation, cells were incubated with 50 µg/ml antibodies for 72 h. Cells were washed twice in ice-cold HBS and lysed in Brij35 buffer (50 mM Tris, 150 mM NaCl, 1 mM $CaCl_2$, 1 mM $MgCl_2$, 1% Brij35, pH 7.4, and protease inhibitor) for 30 min on ice in order to collect non-raft fractions. Cells were scraped and centrifuged at 800 g for 10 min in order to pellet cell debris. Supernatant was centrifuged at 16.000 g for 30 min at 4°C. Pellet was

collected and lysed in Brij58 buffer for cholesterol-rich lipid raft fractions, spun at 16.000 g for additional 30 min. Supernatants of both Brij35- and Brij58 soluble fractions were subjected to immunoprecipitation O/N at 4°C in the presence of specific antibodies and protein A/G magnetic beads. After three washing steps with lysis buffer, the magnetic beads were resuspended in 2x sample buffer (Life Technologies).

For western blotting, cells were lysed in 2x sample buffer, sonicated for 10 sec and proteins were denatured at 95°C for 5 min. Lysates were loaded on 4-12% Bis-Tris PLUS Gels (Thermo Fischer Scientific) for 20 min at 200V and blotted on 0.2 µm pore size PVDF membranes and blocked in 5% milk/TBST for 1h. Blots were incubated with 1:1000 primary antibodies in blocking buffer O/N at 4°C, 3 TBST washing steps and incubated with HRP-conjugated secondary antibodies (Abcam) for 1h at RT. Antigens were visualized with Western Lightning Plus ECL (Perkin-Elmer) using the ChemiDoc imaging system (BioRad).

Matrigel invasion assay

To assess invasion, cells were serum starved for 24h, resuspended in serum-free DMEM in the presence of 50 µg/ml antibodies and seeded in the upper compartment of a 24-wel invasion chamber (BD Biosciences) at 5×10^4 cells/well. The lower compartment was filled with standard culture medium containing 10% serum. Cells were allowed to invade for 48h at 37°C, fixed in 2% formalin and stained with 1% crystal violet for 10 min at RT. Non-invaded cells were removed using a cotton swap; 5 randomly chosen pictures were taken per insert and invaded cells were counted.

Mammosphere and colony formation assay

A single cell suspension was seeded at 500 cells/well in a low-attachment 96 wells plate in mammosphere media (DMEM/F12 phenol-red free, 1% B27, 20 ng/ml hEGF, 20 ng/ml hFGF, 4 µg/ml heparin, 1% pen/strep). Cells were incubated for 14 days at 37°C. Spheroids with an area of >2000 µm^2 were considered as mammospheres and were counted. To calculate mammosphere forming efficiency (MFE), the number of mammospheres were divided by the number of originally seeded cells and expressed as a percentage.

For colony formation assays, 100 cells were seeded in a 6-wells plate in the presence of 50 µg/ml IgG or 10H10 antibody. Cells were incubated for 14 days at 37°C, media was refreshed twice weekly. After 2% formalin fixation and crystal violet visualization, holoclones were counted with a colony density of >50 cells.

Immunofluorescent staining

MDA-MB-231-mfp cells were grown on coverslips in the presence of 50 µg/ml antibody for 72h at 37°C. Cells were washed, fixed with 2% formalin and permeabilized with 0.1% Triton-X100 for 5 min at RT. After 1h in 5% BSA/PBS blocking buffer, primary antibody was applied at 50 µg/ml and incubated overnight at 4°C. After 3 wash steps, cells were incubated with goat anti-rabbit-Alexa-594 (Life Technologies) and phalloidin-FITC (Sigma-Aldrich) for 1h in the dark. Coverslips were mounted with DAPI in ProlongGold (Life Sciences) to stain the nuclei. Images of immunofluorescent labeled cells were captured using a Leica SP5 confocal microscope.

Statistical analysis

Data are represented as mean ± SD. Comparisons between data points were done with Student's t test for two conditions. With three or more data sets significance was calculated using one-way or two-way ANOVA analysis.

4

RESULTS

Tissue factor expression associates with metastasis in Estrogen Receptor negative tumors

We first investigated clinical associations between TF expression and metastasis-free survival of breast cancer patients. Tumor specimens from 574 breast cancer patients were stained for TF and stratified for Estrogen Receptor (ER) expression. Expression of TF in ER-positive tumors did not associate with metastasis-free survival (Fig. 1A). However, a significant association between high TF levels and metastasis in ER-negative tumors was observed that was especially evident in the first five years after diagnosis (Fig. 1B). Cancer stem cells play a fundamental role in metastasis, thus we also determined associations between TF expression and the CSC marker ALDH1; a strong association between high TF expression and ALDH1, was observed (Fig. 1C).

Inhibition of TF signaling reduces metastasis *in vivo*

Our own work in patient material and that in *in vitro* models [10] indicate a role for TF signaling in CSCs and suggest that metastasis may be critically dependent on TF signaling. To further investigate the role of TF signaling in metastasis, the highly aggressive and triple-negative MDA-MB-231-mfp cell line [19] was grafted orthotopically in the mammary
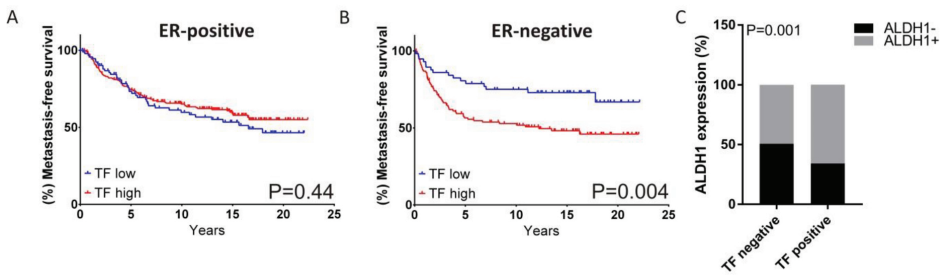
Figure 1 TF expression associates with metastasis-free survival in patients with ER-negative breast tumors, and ALDH1.

(**A**) Kaplan-Meier analysis of metastasis-free survival in breast cancer patients with ER-positive tumors, stratified for TF expression. (**B**) Kaplan-Meier analysis of metastasis-free survival in breast cancer patients with ER-negative tumors, stratified for TF expression. (**C**) Association between the breast cancer stem cell marker ALDH1 and TF expression. Assessments of associations were performed using SPSS and Stata.

gland. In the presence of Mab-10H10 – a specific inhibitor of TF signaling - a 5-fold decrease of tumor growth was observed in comparison to IgG control (Fig. 2A). After mice were sacrificed, lungs were processed to study the presence of human cells using qPCR. Strikingly, the presence of Mab-10H10 reduced metastasis 100-fold (Fig. 2B). The immune system plays a key role in TF-mediated metastasis, as TF deficient cells can only efficiently metastasize in a mouse model that lacks natural killer (NK) cells [20]. To further evaluate the contribution of TF signaling to metastasis, we repeated the *in vivo* experiment in NK cell deficient mice. Tumor volumes were equal after 7 weeks of inoculation (Fig. 2C). In contrast, there was a significant 10-fold reduction of metastasis in the lungs when tumor cells were grafted orthotopically in the presence of Mab-10H10 (Fig. 2D). These data suggest that TF signaling is directly responsible for pro-metastatic events in the primary tumor. Indeed, qPCR analysis of the tumors for EMT-associated markers showed a significant reduction in SNAIL (*SNAI1*) and SLUG (*SNAI2*) mRNA levels, in a NOD-Scid setting (Fig. 2E). While a significant downregulation of *SNAI2* was observed in tumors grown in NK cell deficient mice, *SNAI1* expression remained unaffected and a trend towards decreased *SOX9* expression was present (Fig. 2F). This suggests that inhibition of TF signaling decreases EMT transcription programs *in vivo,* regardless of primary tumor volume.
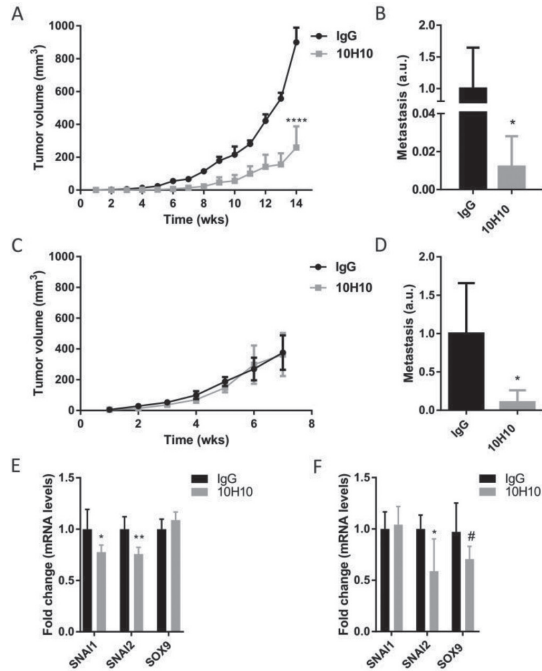
Figure 2 TF signaling inhibition reduces metastasis *in vivo*.

(**A**) MDA-MB-231-mfp cells were orthotopically injected in the presence of 500 ug IgG control or Mab-10H10 antibody in NOD-SCID mice (n=4). Tumor growth was monitored until week 14. Mean and SD are shown. (**B**) Lungs from NOD-SCID mice were analyzed by qPCR to assess metastasis by determining human GAPDH levels corrected for mouse β-actin levels. (**C**) MDA-MB-231-mfp cells were orthotopically injected in the presence of 500 ug IgG control or Mab-10H10 antibody in NOD-SCIDγ mice (n=5). (**D**) Lungs from NOD-SCIDγ mice were analyzed by qPCR to assess metastasis by determining human GAPDH levels corrected for mouse β-actin levels. (**E–F**) Tumors were analyzed by qPCR for the mRNA expression of *SNAI1*, *SNAI2* and *SOX9* from NOD-SCID (**E**) and NOD-SCIDγ mice (**F**). # P <0.10, * P<0.05, **** P <0.0001

Blockade of TF signaling reduces cancer stem cell program *in vitro*

To investigate if blockade of TF signaling resulted in a decreased EMT transcription program *in vitro*, MDA-MB-231-mfp cells were pre-treated with antibodies for 72 hours to inhibit TF signaling. As expected, well-established downstream targets of TF signaling, *CXCL8*, *CXCL1* and *VEGF,* were significantly decreased (Fig. 3A). Although treatment of MDA-MB-231-mfp cells with Mab-10H10 had no effect on *SNAI1* expression, *SNAI2*, *SOX9* and *MMP9* were significantly downregulated by 2-fold at mRNA levels (Fig. 3B, C). Furthermore, similar results

were obtained at antigen levels, with lowered Snail and SOX9 protein levels (Fig. 3D). This attenuated EMT program coincided with a change in morphology, i.e. cells displayed an increased epithelial phenotype compared to cells treated with control IgG (Fig. 3E). Matrix metalloproteinase 9 (MMP9) is a protein involved in the degradation of the extracellular matrix (ECM), allowing tumor cells to escape the primary tumor. In line with reduced *MMP9* mRNA expression levels upon Mab-10H10 treatment, a 2-fold reduction in invasive capacity was observed using matrigel invasion assays compared to control IgG (Fig. 3F). Since SOX9 is considered a driver of cancer stem cell genesis [21] and expression showed a significant decrease in Mab-10H10 treated MDA-MB-231-mfp cells, we hypothesized that these cells would possess diminished CSC properties. Cells were seeded on low attachment plates in order to evaluate mammosphere formation. As expected, the number of tumor colonies were decreased by 2-fold in the Mab-10H10 condition (Fig. 3G). Additionally, Mab-10H10 treated cells showed a similar reduction of holoclone formation (Fig. 3H), being the most aggressive clone-type, with highly proliferative properties and self-renewal capacity [22]. Previously, Endothelial Protein C Receptor, EPCR (encoded by *PROCR*) was described as a CSC marker in triple-negative breast cancer [23]. Likewise, a reduction of *PROCR* was observed when TF signaling was inhibited (Fig. 3I), although no significance could be reached. Thus, inhibition of TF signaling *in vitro* decreases both EMT-associated expression profile and cancer stem cell behavior.

Mab-10H10-treated tumors are less tumorigenic *ex vivo*

To investigate if blockade of TF signaling resulted in a permanent change of malignant tumor cell phenotype, tumors were collected and cultured *ex vivo.* Similar to what was observed with cells treated *in vitro*, tumor cells isolated from Mab-10H10-treated mice showed a morphological change towards an epithelial-like phenotype (Fig. 4A). Ingenuity pathway profiling after gene array analysis indicated alterations in expression profiles that associate with morphology, cellular development, function and cell-to-cell interactions (table S1). This epithelial-like phenotype was supported by an increased expression of the adherens junctions and desmosomes associated genes *JUP* (y-catenin), *PLEKHA7* (pleckstrin) and *DSP* (desmoplakin) - all contributing to epithelial homeostasis (Fig. 4B). Furthermore, expression of EMT markers *SNAI1, SOX9* and *VIM* was decreased in Mab-10H10 *ex vivo* cells (Fig. 4C). Similarly, Snail antigen levels were significantly decreased by 2-fold in Mab-10H10 *ex vivo* cells, while β1 integrin and TF expression remained unchanged (Fig. 4D). Mab-10H10 *ex vivo* cells showed diminished *MMP9* mRNA expression (Fig. 4E). As expected, a significant 8-fold reduction of cell invasion was observed compared to control IgG *ex vivo* cells (Fig. 4F, G). Furthermore, Mab-10H10 *ex vivo* cells had reduced CSC activity, since formation of
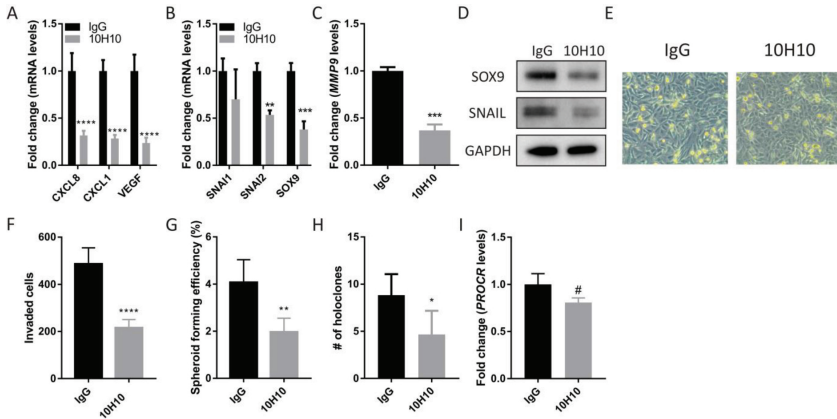
Figure 3 TF signaling inhibition reduces EMT and CSC program *in vitro.*

(**A**) Treatment of MDA-MB-231-mfp cells with 50 µg/ml Mab-10H10 for 72 hours reduces mRNA expression of *CXCL8*, *CXCL1* and *VEGF*. (**B**) Decreased mRNA expression of EMT-associated markers *SNAI1*, *SNAI2* and *SOX9* after 72h treatment with Mab-10H10. (**C**) Mab-10H10 treatment downregulates *MMP9* expression. (**D**) Expression of SOX9 and Snail antigen levels after 72 h antibody treatment. (**E**) Morphological changes were observed during cell culture when cells were treated with 50 µg/ml Mab-10H10. (**F**) Invasion assay of MDA-MB-231-mfp cells in the presence of 50 µg/ml IgG control or Mab-10H10 antibody. (**G**) 500 MDA-MB-31-mfp cells were plated into ultra low-attachment 96-well plates in the presence of 50 µg/ml IgG control or Mab-10H10 antibody and cultured in tumor sphere medium for 14 days. Tumor spheres with a surface larger than 2000 μm^2 were counted. (**H**) Suppressive effect of TF signaling inhibition on colony formation capacity of MDA-MB-231-mfp cells. Colonies consisting over 50 cells with a holo-type phenotype were counted. (**I**) *PROCR* expression after 72 h Mab-10H10 treatment. # P<0.10, *P<0.05, **P<0.01, ***P<0.001, **** P <0.0001

spheroids and holoclones was significantly hampered (Fig. 4H, I). In line with these results, mRNA expression of *PROCR* was also reduced in 10H10 cells (Fig. 4J). Thus, *ex vivo* cells of tumors that had been treated with the TF signaling inhibitor Mab-10H10 display changes in tumor cell phenotype, with decreased EMT and CSC features, that persist during culture *in vitro.*

TF regulates the location of integrins at the plasma membrane

Thus far, we have shown that TF signaling is involved in EMT/CSC programs and in pro-metastatic events. TF influences migration and cell adhesion via the regulation of integrins,
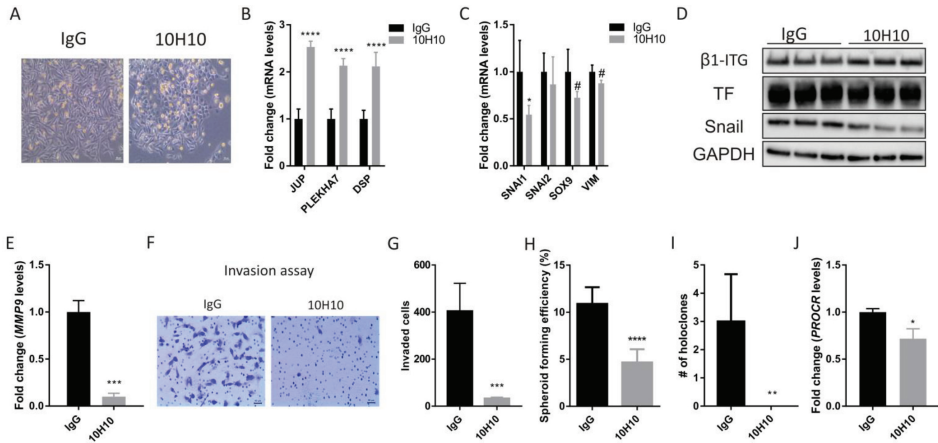
Figure 4 Blockade of TF signaling reduces EMT and CSC program in *ex vivo* cells.
(**A**) Morphological changes were observed during cell culture of *ex vivo* cells that were isolated from tumors. Scale bar = 50 μm. (**B–C**) Transcription levels of adherens junction associated markers *JUP*, *PLEKHA7*, *DSP* (**B**), and EMT-associated markers *SNAI1*, *SNAI2*, *SOX9* and *VIM* (**C**) in IgG or 10H10 *ex vivo* cells measured using qPCR. (**D**) Protein levels in *ex vivo* cells derived from control or Mab-10H10 tumors. (**E**) mRNA level of *MMP9* in IgG and 10H10 *ex vivo* cells. (**F**) Matrigel invasion assay with *ex vivo* IgG and 10H10 cells. Crystal violet staining of invaded cells are shown. (**G**) Data are represented as mean ± SD of cell numbers that invaded in total per well in 4-plo. (**H**) 500 *ex vivo* cells were plated into ultra low-attachment 96-well plates and cultured in tumor sphere medium for 14 days. Tumor sphere numbers were counted with a surface larger than 2000 μm². (**I**) Colonies (>50 cells) with a holoclone phenotype were counted. (**J**) mRNA transcription levels of *PROCR* in IgG or 10H10 *ex vivo* cells. # P <0.15, ***P<0.001, **** P <0.0001

that is independent of PAR2-mediated signaling [13]. Therefore, to unravel the mechanism as to how TF signaling affects CSCs we focused on the interaction with integrins. Since integrins enable the cells to bind ECM, mediate migration and regulate CSCs [24], we addressed whether inhibition of TF signaling influences integrin behavior. First, we investigated the effects of integrin activation on EMT programs using different extracellular matrix (ECM) components, i.e. vitronectin that binds αvβ3 integrin [25] and laminin, a ligand for many β1 integrin dimers and α6β4 integrin [26]. Cells were seeded on vitronectin or laminin-coated plates and treated with Mab-10H10 for 72 hours, followed by mRNA analysis of EMT-associated factors. A 2-fold reduction of *SNAI1* and *SNAI2* expression was found when TF signaling was inhibited in cells on vitronectin coated plates, while expression remained equal
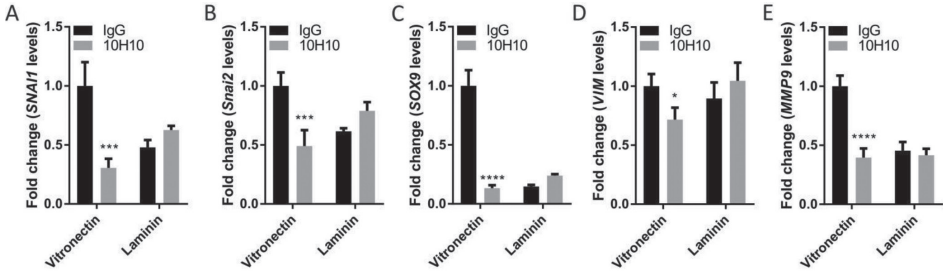
Figure 5 Vitronectin and laminin contribute to different EMT and CSC program in *in vitro* cells.

Transcription levels of *SNAI1* (**A**), *SNAI2* (**B**), *SOX9* (**C**), *VIM* (**D**) and *MMP9* (**E**) in MDA-MB-231-mfp cells in the presence of IgG control or 10H10 antibodies for 72 hours on vitronectin or laminin coated plates. *P<0.05, ***P<0.001, **** P <0.0001

when cells were seeded on laminin (Fig. 5A, B). The effects of different ECM components on *SOX9* mRNA expression were even more pronounced, with a 90% reduction, on vitronectin, (Fig. 5C). Similar trends were observed with respect to *VIM* and *MMP9* expression after treatment with 10H10 on vitronectin but not on laminin as an ECM component (Fig. 5D, E).

Next, we further investigated how integrins influence TF signaling mediated EMT- and CSC-associated behavior. Cells were treated with Mab-10H10 for 72 hours, subsequently lysed in Brij35-buffer that dissolves non-raft, cholesterol-poor cell membrane fractions [27]. β1 integrins were immunoprecipitated with various β1 integrin conformation-recognizing antibodies, after which precipitates were analyzed for β1 integrin and TF. Inhibition of TF signaling resulted in an approximately 2-fold reduction of TF/β1 integrin complexes in the Brij35-soluble fraction (Fig. 6A), while β1 integrin expression remained equal. Interestingly, pull down assays with AIIB2 (total β1 integrin) and HUTS21 (active β1 integrin) co-immunoprecipitated FAK and Src when MDA-MB-231-mfp cells were treated with Mab-10H10, suggesting an active β1 integrin conformation. The β1 integrin antibody TS2/16, that activates β1 on intact cells and immunoprecipitates the TF-FVIIa complex [28], did not immunoprecipitate FAK/Src in the presence of Mab-10H10,indicating that FVIIa is not involved in the antibody effect. In addition, immunofluorescent staining for FAK in MDA-MB-231-mfp cells treated with Mab-10H10 demonstrated the formation of focal adhesions at the plasma membrane (Fig. 6B), confirming FAK activation in the presence of Mab-10H10. Inhibition of FAK resulted in a significant increase of *SNAI1/2* expression, while *SOX9* remained unaffected (Fig. 6C). Mab-10H10 treatment decreased α2 and α3 integrin heterodimers with β1

integrin and co-precipitating TF in the Brij35-soluble fraction (Fig. 6D). In contrast, pre-cipitation of TF/β1 integrin was increased markedly by Mab-10H10 treatment in the α6 in-tegrin pull down from cholesterol-rich membrane fraction − Brij-58 soluble − and less so in the non-raft fractions. Total expression of alpha-integrin subunits did not change upon Mab-10H10 treatment (Fig. 6E). These data suggest that blockade of TF signaling causes a shift of TF towards α6β4 integrin into the cholesterol-rich membrane fractions. These data also indicate that integrin activation is induced by Mab-10H10 treatment to suppress the CSC phenotypes. Consistently, inhibition of β1 integrin − but not PAR2 − increased mam-mosphere formation in cells treated with Mab-10H10 (Fig. 6F). Treatment of MDA-MB-231-mfp cells with the PAR2 antagonist GB83 showed similar results as those observed after antibody-mediated inhibition (Fig. 6G). Additionally, mRNA expression profiles of EMT-related genes were examined after inhibition of β1 integrin and PAR2. Inhibition of either receptor resulted in increased *SNAI2* expression. A trend towards increased *SOX9* expression was observed when β1 integrin was inhibited with Mab-AIIB2, while inhibition of PAR2 had no effect on *SOX9* transcription levels (fig. 6H). These data suggest that TF signaling mediates the localization and function of β1 integrin on the cell membrane. Fur-thermore, disruption of the TF/β1 integrin complex results in an epithelial-like morphology with less tumorigenic properties.

TF signaling keeps cells in a mesenchymal state via suppression of β4 integrin expression

How integrins contribute to cancer stem cell behavior is as yet obscure. Recently, Bierie and co-workers showed that α6β4 integrin distinguishes subpopulations in mesenchymal triple negative breast cancer [29]. Cells that are β4 integrin positive in MDA-MB-231 associated with a more epithelial morphology and decreased tumorigenic properties. We found that treatment with Mab 10H10 influenced β4 integrin expression in our highly aggressive MDA-MB-231-mfp cell line. After 72 hours Mab-10H10 treatment, magnetic activated cell sorting (MACS) isolated the same number of β1 integrin positive cells (Fig. 7A), but TF signaling inhibition increased the number of cells that express β4 integrin 15-fold (Fig. 7B). After MACS sorting these cells were cultured for 1 week. Whereas the cells displaying low integrin β4 expression from control IgG treated cells had mesenchymal-like morphology, an epi-thelial-like morphology was observed in the β4 integrin[high] population isolated from Mab-10H10-treated cells (Fig. 7C). Immunoprecipitation of β4 integrin confirmed the increased association of α6 integrin and TF in Mab-10H10 treated cells. Furthermore, increased FAK and Src antigen were co-precipitated with integrin β4 after Mab-10H10 treatment (Fig. 7D). Diminished TF signaling caused a morphological change into less tumorigenic cells via in-
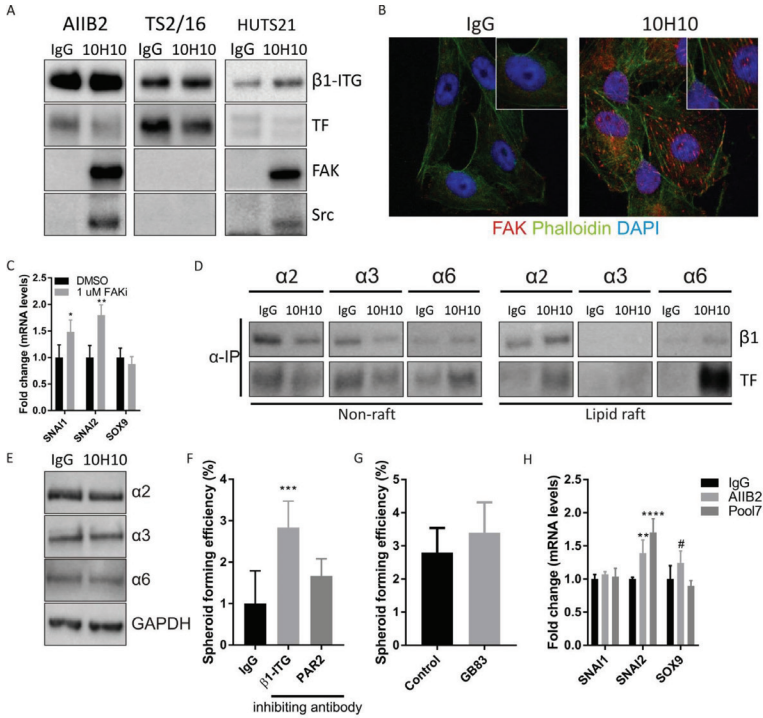
Integrin regulation by Tissue Factor promotes cancer stemness and metastasis in breast cancer.

Figure 6 TF determines β1 integrin localization on the cell membrane.

(**A**) Pull down assay of β1 integrins with AIIB2, TS2/16 and HUTS21 after 72h treatment with IgG or Mab-10H10. Co-immunoprecipitation was analyzed with Western Blot for β1 integrin, TF, FAK and Src. (**B**) Blockade of TF signaling increases focal adhesion complex formation after 72 h Mab-10H10 treatment. MDA-MB-231-mfp cells were permeabilized and stained for FAK. (**C**) mRNA expression of *SNAI1, SNAI2* and *SOX9* in MDA-MB-231-mfp cells after 72h treatment with control (DMSO) or 1 uM FAK II inhibitor. (**D**) Localization of α2, α3 and α6 integrin was studied in non-raft and lipid raft fractions after 72h 10H10 treatment. Precipitates were analyzed for the presence of β1 integrin and TF on Western Blot. (**E**) Western blotting for α-integrin subunits on total cell lysates of MDA-MB-231-mfp cells showed no changes in antigen levels after blockade of TF signaling. (**F**) 500 MDA-MB-231-mfp cells were plated into ultra low-attachment 96-well plates in the presence of 50 µg/ml control IgG, Mab-AIIB2 (β1 integrin) or Pab-pool7 (PAR2) antibody and cultured in tumor sphere medium for 14 days. Tumor spheres with a surface larger than 2000 µm^2 were counted. (**G**) 500 cells were plated into ultra low-attachment 96-well plates in the presence of control (DMSO) or 10 µM PAR2 antagonist (GB83) and cultured in tumor sphere medium for 14 days. Tumor sphere numbers were counted with a surface larger than 2000 um^2. (**H**) Transcription levels of *SNAI1, SNAI2* and *SOX9* in MDA-MB-231-mfp cells in the presence of control IgG, Mab-AIIB2 (β1 integrin) or Pab-pool7 (PAR2) antibody for 72 hours.
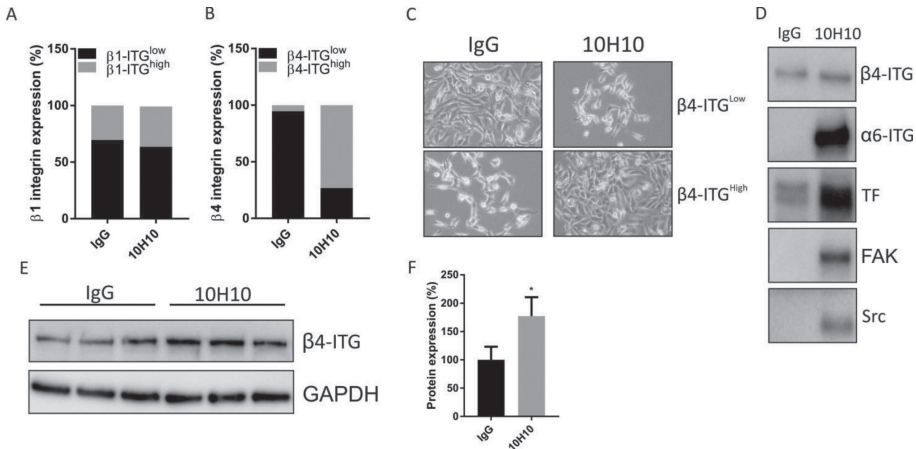
Figure 7 Inhibition of TF signaling increases expression and crosstalk with $\alpha6\beta4$ integrin. (A-B)

Cells were treated with IgG or 10H10 antibody for 72 h and sorted with MACS antibodies recognizing $\beta1$ (**A**) or $\beta4$ integrin (**B**) expression. Table represents relative percentage of $\beta1$ and $\beta4$ integrin low and high expression. (**C**) One week of cell culture after MACS sorting show morphological changes in $\beta4$ integrin[High] cells. (**D**) Pull down assay for $\beta4$ integrin after Mab-10H10 confirms complex formation with $\alpha6$ integrin subunit, TF, FAK and Src in MDA-MB-231-mfp cells. (**E**) Protein expression analysis of $\beta4$ integrin in IgG and 10H10 *ex vivo* cells. (**F**) Band intensity was quantified using ImageJ software. *P<0.05

creased $\alpha6\beta4$ integrin expression and activation at the cell surface. Interestingly, $\beta4$ integrin expression was twice as high in 10H10 *ex vivo* cells (Fig. 7E, F), whereas TF and $\beta1$ integrin expression remained unchanged (Fig. 4D).

DISCUSSION

Here, we show that TF expression negatively associates with metastasis-free survival in ER-negative breast tumors. We also demonstrate in orthotopic xenograft mouse models that TF signaling influences epithelial to mesenchymal transition, cancer stem cell programs and metastasis that is independent of NK cells. Finally, we show that TF regulates integrin function, focal adhesion complexes and adherens junction components resulting in an epithelial cell morphology. Based on these data we conclude that TF signaling maintains breast cancer cells in a mesenchymal state by suppressing epithelial features, thus promoting CSC generation and a pro-metastatic state (Fig. 8).

TF expression has been linked to decreased metastasis-free survival in lung, gastric, pancreatic and colorectal cancer [30-33], but associations between TF and metastasis in breast cancer patients have remained obscure [34-36]. In this study an association could be found when breast tumors were stratified for ER status, with a significant association in ER-negative tumors. Surprisingly, such an association was not found in tumors from breast cancer patients with ER-positive tumors, possibly reflecting the different biological and clinical characteristics of these breast tumor types. In support, a recent study demonstrates increased TF expression in triple-negative breast cancer [37], a highly invasive subtype of breast cancer that is associated with poor survival [38]. Of note, in our work we used MDA-MB-231-mfp cells constituting a triple-negative breast cancer cell line and in these cells TF supports invasion and metastasis in an ER$^-$ setting.

When MDA-MB-231-mfp cells were orthotopically grafted in the presence of the TF signaling inhibitor Mab-10H10 a dramatic decrease in lung metastasis was observed. As this antibody does not inhibit coagulant properties of TF, our results demonstrate that in an orthotopic setting, TF signaling impacts metastasis. It should also be noted that TF signaling promoted metastasis both in murine models harboring NK cells and models lacking NK cells. This is of importance as previous work making use of experimental metastasis models – relying on injection of cancer cells into the bloodstream – suggested that in this setting evasion of NK cells was dependent on coagulant function of TF. Nevertheless, experimental metastasis does not fully recapitulate the metastatic process as primary tumor growth, degradation of the basement membrane, local invasion and intravasation into the bloodstream are circumvented [39]. One other outcome of our *in vivo* work is that primary tumor growth was unaffected by Mab-10H10 treatment in the absence of NK cells. This raises the possibility that Mab-10H10 treatment in NK proficient mouse models primarily mediates antibody-dependent cellular cytotoxicity (ADCC) [15, 40].

We next questioned why inhibition of TF signaling had such an impact on metastasis and reasoned that Mab-10H10 treatment influenced metastatic potential of the primary tumor cells. Our experiments using *in vitro* and *ex vivo* approaches demonstrated that TF signaling affects early metastatic events such as maintenance of an EMT-program in tumors. Mab-10H10 treatment resulted in a downregulation of EMT transcription factors Snail and/or Slug. As TF appears to influence EMT, which is dynamically linked to cancer stem cells [10], and as expression of the cancer stem cell effector SOX9 was significantly reduced in our *in vitro* model after Mab-10H10 treatment, the question raised whether TF expression is associated with CSCs. Indeed, our clinical data demonstrates an association between high

TF levels and ALDH1, a marker for CSCs. In support, Mab-10H10 treatment resulted in decreased mammosphere formation and holoclone formation, suggesting that specifically TF signaling influences cancer stem cells. Shaker et al. have previously demonstrated that TF expression promotes CSCs in breast cancer, nevertheless, our study is the first to show that the involvement of TF in CSC maintenance is dependent on its signaling properties. Collectively, these data show that TF signaling is directly responsible for NK-independent metastasis via modulation of the EMT and CSC program.

Unfortunately, insights into effects of Mab-10H10 on CSC-associated markers remained limited in this study. $CD44^+/CD24^-$ is classically regarded as a CSC signature, but MDA-MB-231-mfp cells are enriched in $CD44^+/CD24^-$ (>90%) and ALDH1, another proposed marker for CSCs is hardly detected in MDA-MB-231-mfp cells [23]. Schaffner et al. previously demonstrated that EPCR may serve as a marker for CSCs in MDA-MB-231-mfp cells [23]. In our model, *PROCR* transcript levels were significantly downregulated in Mab-10H10 *ex vivo* cells, whereas only a trend was observed in Mab-10H10 treated *in vitro* cells. Unfortunately, no differences on EPCR surface expression could be observed using flow cytometry (data not shown). Hwang-Verslues et al. previously suggested that EPCR as a CSC marker on itself is a weak biomarker in breast cancer cell lines [41]. Rather we found that β4 integrin expression, which was recently shown by Bierie et al. to be a negative marker for CSCs, discriminated between aggressive and less aggressive Mab-10H10-treated cells [29]. It should be noted that the study by Bierie et al., like ours, did not find differences in *PROCR* expression when comparing integrin $β4^{high}$ MDA-MB-231 cells with integrin $β4^{low}$ cells.

An interesting observation in this study was the change in morphology of 10H10-treated cells from a mesenchymal to an epithelial-like phenotype both *in vitro* and *ex vivo* concomitant with elevated β4 integrin expression. Furthermore, our 10H10-treated *ex vivo* cell model demonstrated increased expression profiles of adherens junction and desmosome components again reflective of an epithelial-like state. Despite these apparent changes in morphology, we were unable to show significant changes in EMT-related transcriptional programs in our 10H10-treated *ex vivo* cells as opposed to those observed in our *in vitro* model, where only *SNAI1* and *SOX9* expression were affected. Although these data appear to be in conflict, we hypothesize that the tumor microenvironment may have influenced the EMT state of our ex vivo cells. A recent study shows that cells undergo several intermediate stages during EMT and that these stages are determined by the presence of stromal cells [42]. Indeed, Magnus et al. reported previously that tumor cell TF expression and the microenvironment dynamically regulate each other [43]. Therefore, we hypothesize that

in vitro Mab-10H10 treatment skews tumor cells towards a transition state to MET (mesenchymal-to-epithelial transformation), while *ex vivo* cells derived from 10H10 tumors, influenced by the tumor microenvironment, have fully undergone MET. Thus, TF signaling appears to be required for the initial transformation and the microenvironment further directs a full MET transition.

TF signaling may occur via multiple receptors. Classically, TF mediates FVIIa-dependent activation of PAR2, however, inhibition of PAR2 did not impact spheroid forming efficiency. In addition, we performed our experiments in the absence of FVIIa making it unlikely that TF-dependent effects on EMT/CSC are FVIIa- or PAR2-mediated, although we have not investigated this extensively. Rather, we postulate that TF, in the context of EMT and CSC biology, regulates integrin function. Indeed, we observed that EMT/CSC-associated markers were downregulated when TF/integrin crosstalk was inhibited with 10H10 on vitronectin, an activator of β3 and β5 integrins [44]. In contrast, expression of these markers was already low when cells were seeded on laminin a ligand for β1 integrin [45], and expression was not further downregulated when TF signaling was inhibited. In addition, inhibition of β1 integrin resulted in increased *SNAI2* and *SOX9* expression, whereas inhibition of PAR2 only affected transcription levels of *SNAI2.* These data suggest that β1 integrin is involved in TF signaling-dependent EMT and CSC transcriptional programs. Altogether, we hypothesize that TF/PAR-mediated signaling is required for angiogenesis and proliferation, while the TF/integrin axis is responsible for EMT and CSC.

To further unravel the nature of the β1 integrin/TF signaling pathway, β1 integrin immunoprecipitates were investigated. Mab-10H10 led to uncoupling of TF/β1 integrin complexes, as shown in this study and previous studies. Furthermore, in the presence of 10H10 increased binding of focal adhesion kinase to β1 integrin was observed, as well as increases in focal adhesion complexes and presence of actin fibers. This may be initiated by Mab-10H10 that shifts TF in a complex with α6β1 integrin – which may not be recognized by TS2/16 – and recruits filamin and FAK through the cytoplasmic domain [46]. Further, this Mab-10H10 treatment resulted in an increase of the active β1 integrin conformation and a decrease in cancer stemness. Although α6β1 integrin has been implicated in CSC phenotypes [47], our data show that TF dictates FAK/Src recruitment to any α6 integrin heterodimer – including α6β4 integrin – that promotes differentiation. Thus, we postulate that 10H10 reverses TF-dependent inhibition of β1 integrin, leading to focal adhesion assembly and an epithelial state.

4

The epithelial morphology may be further influenced by β4 integrin [48], and others have shown that an interaction of α6β4 integrin with CD151 increases cell adhesion and formation of hemidesmosomes, that mediates a stable cell attachment to the ECM [49]. Indeed, we observed a significant increase in cellular β4 integrin expression upon inhibition of TF signaling. Furthermore, we have observed a physical interaction between TF and β4 integrin. It is tempting to speculate that the TF/β4 integrin complex is actively involved in the transition to an epithelial state and CSC differentiation. Therefore, it would be of interest to further elucidate the nature of the TF/β4 integrin signaling axis and its impact on hemidesmosome assembly.

In conclusion, uncoupling of TF/β1 integrin signaling pathways, increases integrin β4 expression, decreases EMT/CSC programs, resulting in diminished lung metastases. This study shows that TF signaling may be an important target for the treatment of triple negative breast cancer, and TF/β1 interactions may be targeted to prevent relapse and increase overall survival.

Integrin regulation by Tissue Factor promotes cancer stemness and metastasis in breast cancer.
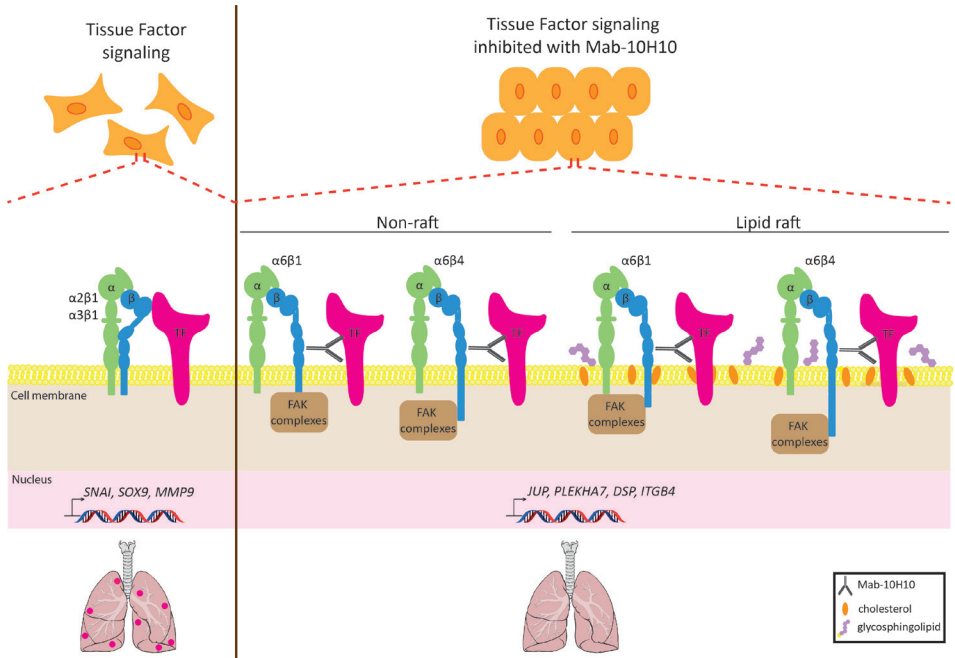

Figure 8 Schematic overview.

Inhibition of TF signaling with Mab-10H10 results in an epithelial morphology, with less CSC behavior and metastasis to the lungs. The proposed mechanism comprises disruption of TF/β1 integrin complexes, an increase in β4 integrin expression and formation of focal adhesion complexes by α6β1 and α6β4 integrins.

4

ACKNOWLEDGEMENTS

REFERENCES

1. DeSantis, C.E., et al., *Breast cancer statistics, 2017, racial disparity in mortality by state.* CA Cancer J Clin, 2017. **67**(6): p. 439-448.

2. Kim, D.H., et al., *Epithelial Mesenchymal Transition in Embryonic Development, Tissue Repair and Cancer: A Comprehensive Overview.* J Clin Med, 2017. **7**(1).

3. Lamouille, S., J. Xu, and R. Derynck, *Molecular mechanisms of epithelial-mesenchymal transition.* Nat Rev Mol Cell Biol, 2014. **15**(3): p. 178-96.

4. Garg, M., *Epithelial plasticity and cancer stem cells: Major mechanisms of cancer pathogenesis and therapy resistance.* World J Stem Cells, 2017. **9**(8): p. 118-126.

5. Ishiwata, T., *Cancer stem cells and epithelial-mesenchymal transition: Novel therapeutic targets for cancer.* Pathol Int, 2016. **66**(11): p. 601-608.

6. Kotiyal, S. and S. Bhattacharya, *Breast cancer stem cells, EMT and therapeutic targets.* Biochem Biophys Res Commun, 2014. **453**(1): p. 112-6.

7. Gupta, P.B., C.L. Chaffer, and R.A. Weinberg, *Cancer stem cells: mirage or reality?* Nat Med, 2009. **15**(9): p. 1010-2.

8. A, D.A.C.P. and C. Lopes, *Implications of Different Cancer Stem Cell Phenotypes in Breast Cancer.* Anticancer Res, 2017. **37**(5): p. 2173-2183.

9. Shibue, T. and R.A. Weinberg, *EMT, CSCs, and drug resistance: the mechanistic link and clinical implications.* Nat Rev Clin Oncol, 2017. **14**(10): p. 611-629.

10. Shaker, H., et al., *Tissue Factor promotes breast cancer stem cell activity in vitro.* Oncotarget, 2017. **8**(16): p. 25915-25927.

11. van den Berg, Y.W., et al., *The relationship between tissue factor and cancer progression: insights from bench and bedside.* Blood, 2012. **119**(4): p. 924-32.

12. Dorfleutner, A., et al., *Cross-talk of integrin alpha3beta1 and tissue factor in cell migration.* Mol Biol Cell, 2004. **15**(10): p. 4416-25.

13. Kocaturk, B. and H.H. Versteeg, *Tissue factor-integrin interactions in cancer and thrombosis: every Jack has his Jill.* J Thromb Haemost, 2013. **11 Suppl 1**: p. 285-93.

14. Ahamed, J., et al., *Disulfide isomerization switches tissue factor from coagulation to cell signaling.* Proc Natl Acad Sci U S A, 2006. **103**(38): p. 13932-7.

15. Versteeg, H.H., et al., *Inhibition of tissue factor signaling suppresses tumor growth.* Blood, 2008. **111**(1): p. 190-9.

16. van Nes, J.G., et al., *COX2 expression in prognosis and in prediction to endocrine therapy in early breast cancer patients.* Breast Cancer Res Treat, 2011. **125**(3): p. 671-85.

17. Kocaturk, B., et al., *Alternatively spliced tissue factor promotes breast cancer growth in a beta1 integrin-dependent manner.* Proc Natl Acad Sci U S A, 2013. **110**(28): p. 11517-22.

18. Kocaturk, B. and H.H. Versteeg, *Orthotopic injection of breast cancer cells into the mammary fat pad of mice to study tumor growth.* J Vis Exp, 2015(96).

19. Jessani, N., et al., *Carcinoma and stromal enzyme activity profiles associated with breast tumor growth in vivo.* Proc Natl Acad Sci U S A, 2004. **101**(38): p. 13756-61.

20. Palumbo, J.S., et al., *Tumor cell-associated tissue factor and circulating hemostatic factors cooperate to increase metastatic potential through natural killer cell-dependent and-independent mechanisms.* Blood, 2007. **110**(1): p. 133-41.

21. Guo, W., et al., *Slug and Sox9 cooperatively determine the mammary stem cell state.* Cell, 2012. **148**(5): p. 1015-28.

4

22.   Beaver, C.M., A. Ahmed, and J.R. Masters, *Clonogenicity: holoclones and meroclones contain stem cells.* PLoS One, 2014. **9**(2): p. e89834.

23.   Schaffner, F., et al., *Endothelial protein C receptor function in murine and human breast cancer development.* PLoS One, 2013. **8**(4): p. e61071.

24.   Seguin, L., et al., *Integrins and cancer: regulators of cancer stemness, metastasis, and drug resistance.* Trends Cell Biol, 2015. **25**(4): p. 234-40.

25.   Horton, M.A., *The alpha v beta 3 integrin "vitronectin receptor".* Int J Biochem Cell Biol, 1997. **29**(5): p. 721-5.

26.   Belkin, A.M. and M.A. Stepp, *Integrins as receptors for laminins.* Microsc Res Tech, 2000. **51**(3): p. 280-301.

27.   Marwali, M.R., et al., *Membrane cholesterol regulates LFA-1 function and lipid raft heterogeneity.* Blood, 2003. **102**(1): p. 215-22.

28.   Rothmeier, A.S., et al., *Identification of the integrin-binding site on coagulation factor VIIa required for proangiogenic PAR2 signaling.* Blood, 2018. **131**(6): p. 674-685.

29.   Bierie, B., et al., *Integrin-beta4 identifies cancer stem cell-enriched populations of partially mesenchymal carcinoma cells.* Proc Natl Acad Sci U S A, 2017. **114**(12): p. E2337-E2346.

30.   Sawada, M., et al., *Expression of tissue factor in non-small-cell lung cancers and its relationship to metastasis.* Br J Cancer, 1999. **79**(3-4): p. 472-7.

31.   Yamashita, H., et al., *Tissue factor expression is a clinical indicator of lymphatic metastasis and poor prognosis in gastric cancer with intestinal phenotype.* J Surg Oncol, 2007. **95**(4): p. 324-31.

32.   Nitori, N., et al., *Prognostic significance of tissue factor in pancreatic ductal adenocarcinoma.* Clin Cancer Res, 2005. **11**(7): p. 2531-9.

33.   Seto, S., et al., *Tissue factor expression in human colorectal carcinoma: correlation with hepatic metastasis and impact on prognosis.* Cancer, 2000. **88**(2): p. 295-301.

34.   Sturm, U., et al., *Immunohistological detection of tissue factor in normal and abnormal human mammary glands using monoclonal antibodies.* Virchows Arch A Pathol Anat Histopathol, 1992. **421**(2): p. 79-86.

35.   Ueno, T., et al., *Tissue factor expression in breast cancer tissues: its correlation with prognosis and plasma concentration.* Br J Cancer, 2000. **83**(2): p. 164-70.

36.   Ryden, L., et al., *Evidence for tissue factor phosphorylation and its correlation with protease-activated receptor expression and the prognosis of primary breast cancer.* Int J Cancer, 2010. **126**(10): p. 2330-40.

37.   Zhang, X., et al., *Pathological expression of tissue factor confers promising antitumor response to a novel therapeutic antibody SC1 in triple negative breast cancer and pancreatic adenocarcinoma.* Oncotarget, 2017. **8**(35): p. 59086-59102.

38.   Foulkes, W.D., I.E. Smith, and J.S. Reis-Filho, *Triple-negative breast cancer.* N Engl J Med, 2010. **363**(20): p. 1938-48.

39.   Valastyan, S. and R.A. Weinberg, *Tumor metastasis: molecular insights and evolving paradigms.* Cell, 2011. **147**(2): p. 275-92.

40.   Richards, J.O., et al., *NK cell-mediated antibody-dependent cellular cytotoxicity is enhanced by tamoxifen in HER2/neu non-amplified, but not HER2/neu-amplified, breast cancer cells.* Cancer Immunol Immunother, 2016. **65**(11): p. 1325-1335.

41.   Hwang-Verslues, W.W., et al., *Multiple lineages of human breast cancer stem/progenitor cells identified by profiling with stem cell markers.* PLoS One, 2009. **4**(12): p. e8377.

42.   Pastushenko, I., et al., *Identification of the tumour transition states occurring during EMT.* Nature, 2018. **556**(7702): p. 463-468.

43. Magnus, N., et al., *Tissue factor expression provokes escape from tumor dormancy and leads to genomic alterations.* Proc Natl Acad Sci U S A, 2014. **111**(9): p. 3544-9.

44. Yilmaz, M. and G. Christofori, *EMT, the cytoskeleton, and cancer cell invasion.* Cancer Metastasis Rev, 2009. **28**(1-2): p. 15-33.

45. Chen, Q.K., et al., *Extracellular matrix proteins regulate epithelial-mesenchymal transition in mammary epithelial cells.* Differentiation, 2013. **86**(3): p. 126-32.

46. Ott, I., et al., *A role for tissue factor in cell adhesion and migration mediated by interaction with actin-binding protein 280.* J Cell Biol, 1998. **140**(5): p. 1241-53.

47. Goel, H.L., et al., *GLI1 regulates a novel neuropilin-2/alpha6beta1 integrin based autocrine pathway that contributes to breast cancer initiation.* EMBO Mol Med, 2013. **5**(4): p. 488-508.

48. Nistico, P., et al., *beta1 and beta4 integrins: from breast development to clinical practice.* Breast Cancer Res, 2014. **16**(5): p. 459.

49. Levy, S. and T. Shoham, *Protein-protein interactions in the tetraspanin web.* Physiology (Bethesda), 2005. **20**: p. 218-24.

4

SUPPLEMENTARY MATERIALS

Table S1

Summary of Ingenuity pathway analysis on 10H10 *ex vivo* cells.

10H10 *ex vivo* cells	
Top canonical pathways	
	p-value
ERK5 signaling	8,99E-06
Protein ubiquitination pathway	5,22E-05
Antigen presentation pathway	1,23E-04
Virus entry via endocytic pathways	1,29E-04
Fcy receptor-mediated phagocytosis in macrophages and monocytes	1,32E-04
Molecular and cellular functions	
	p-value range
Cellular growth and proliferation	8,91E-03 - 7,00E-19
Cell death and survival	9,81E-03 - 6,74E-11
Protein synthesis	9,80E-03 - 5,76E09
Cellular movement	9,45E-03 - 5,83E-09
Cellular development	8,91E-03 - 3,40E-07
Top Upstream regulators	
	p-value of overlap
EZH2	4,72E-14
TNF	1,52E-12
SND1	5,58E-10
TREM1	1,60E-09
TP63	2,24E-09
Top networks	
Cell morphology, cellular assembly and organization, cellular function and maintenance	
Dermatological diseases and conditions, organismal injury and abnormalities, cellular function and maintenance	
Post-translational modification, cell-to-cell signaling and interaction, hair and skin development and function	
Cell death and survival, organismal injury and abnormalities, protein synthesis	
Organismal development, cell death and survival, cellular development	

Table S2

qPCR primer sequences.

Gene	Primer sequence		
SNAI1	Forward 5'–	CCCCAATCGGAAGCCTAACT	–3'
	Reverse 5'–	GCTGGAAGGTAAACTCTGGATTAGA	–3'
SNAI2	Forward 5'–	TGTTGCAGTGAGGGCAAGAA	–3'
	Reverse 5'–	GACCCTGGTTGCTTCAAGGA	–3'
SOX9	Forward 5'–	CTCTGGAGACTTCTGAACG	–3'
	Reverse 5'–	AGATGTGCGTCTGCTC	–3'
CXCL8	Forward 5'–	AGGTGCAGTTTTGCCAAGGA	–3'
	Reverse 5'–	TTTCTGTGTTGGCGCAGTGT	–3'
CXCL1	Forward 5'–	AGTCATAGCCACACTCAAGAATGG	–3'
	Reverse 5'–	GATGCAGGATTGAGGCAAGC	–3'
VEGF	Forward 5'–	CTCCACCATGCCAAGTGGTC	–3'
	Reverse 5'–	CTCGATTGGATGGCAGTAGCT	–3'
JUP	Forward 5'–	CAAGAACAACCCCAAGTTC	–3'
	Reverse 5'–	ATGATCAGCTTGCTCTCC	–3'
PLEKHA7	Forward 5'–	AAGACCAGCTAGAATCTGTG	–3'
	Reverse 5'–	CACATCATTCTCCAACTTCA	–3'
DSP	Forward 5'–	GAGATGGAATACAACTGAC	–3'
	Reverse 5'–	CCTTTTCTGGTAAGCATCAC	–3'
VIM	Forward 5'–	GGAAACTAATCTGGATTCACTC	–3'
	Reverse 5'–	CATCTCTAGTTTCAACCGTC	–3'
m β–ACTIN	Forward 5'–	AGGTCATCACTATTGGCAACGA	–3'
	Reverse 5'–	CCAAGAAGGAAGGCTGGAAAA	–3'
hGAPDH	Forward 5'–	TTCCAGGAGCGAGATCCCT	–3'
	Reverse 5'–	CACCCATGACGAACATGGG	–3'

4